Development and Application of Information Resources for Education and Teaching of Yarn History Based on 5G Network Technology

Xiaoming Yang (sd7980@126.com)
Donghua University

Research Article

Keywords: Fifth generation (5G), Yarn education, Grayscale transformation, Multi-resolution Markov Random Field (MRMRF) model, Fourier transform, Two scale attention model, Improved Support Vector Machine (ISVM), Improved Particle Swarm Optimization (IPSO) algorithm

Posted Date: May 20th, 2022

DOI: https://doi.org/10.21203/rs.3.rs-1052534/v1

DEVELOPMENT AND APPLICATION OF INFORMATION RESOURCES FOR EDUCATION AND TEACHING OF YARN HISTORY BASED ON 5G NETWORK TECHNOLOGY

Wen Zhang [1], Xiaoming Yang [2,]
1College of Humanities, Donghua University, Changning, Shanghai, China
2College of Humanities, Donghua University, Changning, Shanghai, China

***Correspondence Author: Xiaoming Yang, Email: sd7980@126.com**

Abstract:

Yarn education is a crucial step in producing high-quality textile end products. Online yarn testing can reduce latency in necessary process control by providing rapid insights into yarn quality, leading to the production of superior quality yarns. This paper proposes the development and application of information resources for the education and teaching of yarn history based on fifth-generation (5G) network technologies. Initially, the yarn database is preprocessed using Grayscale transformation and image filtering methods. Secondly, yarn segmentation is implemented using a Multi-resolution Markov Random Field (MRMRF) model. The statistical and relative features are extracted using Fourier transform and two-scale attention model respectively. We propose Improved Support Vector Machine (ISVM) classification for classifying the yarn images. The 5G network is initialized and Transmission Control Protocol is used for data transfer. To enhance the performance we propose an Improved Particle Swarm Optimization (IPSO) algorithm. The performance of the suggested methodology is analyzed and compared with existing methodologies using the MATLAB simulation tool. The classification performance of the proposed algorithm indicates that the 5G framework might provide an accurate, fast, reliable, and cost-effective solution to industrial automation.

Keywords: **Fifth generation (5G), Yarn education, Grayscale transformation, Multi-resolution Markov Random Field (MRMRF) model, Fourier transform, Two scale attention model, Improved Support Vector Machine (ISVM), Improved Particle Swarm Optimization (IPSO) algorithm**

I. INTRODUCTION

Cotton materials are organically sourced materials that we utilize regularly. The hydrate pattern and process in cotton, as well as the major component, cellulose, and associated components, have been widely investigated since the water content affects the architecture and physicochemical characteristics. Yet,

because water particles interact with neighboring molecules to generate distinct water structures, observing and studying those activities in depth is hard, and numerous methodologies are still necessary [1].

The use of 4 categories of the Kawabata Evaluation System (KES) in measuring the fabric's tensile, shear, bending, compression, and surface qualities is the most often utilized objective evaluation of this component of comfort in fabrics. Many researchers have been studying the sensory evaluation of tactile qualities of fabrics for years, and it is still important and has space for development. Sensorial comfort encompasses all low-stress mechanical qualities such as tensile, shear, straight bending, and compressive behaviors, as well as waviness and friction, which are all critical criteria. One of the most essential qualities influencing the pliability, and handling of woven fabrics is the shear mechanism. Fabric compressing qualities are influenced by a variety of factors, including the compression properties of the constituent yarns. The textile materials, which comprise fiber composition, yarn characteristics, fabric structure, and finishing processes, influence the sensory comfort of clothes [2].

Based on fifth-generation (5G) network technology, this article proposes the development and deployment of information resources for education and teaching of yarn history. Grayscale transformation and picture filtering procedures are used to preprocess the yarn database at first. A Multi-resolution Markov Random Field (MRMRF) model is used to accomplish yarn segmentation. Fourier transform and two-scale attention models are used to extract statistical and relative characteristics, respectively. For classifying the yarn photos, we propose using Improved Support Vector Machine (ISVM) classification. The 5G network has been set up, and data is transferred using the Transmission Control Protocol. We present the Improved Particle Swarm Optimization (IPSO) technique to improve performance. Using the MATLAB simulation tool, the suggested methodology's performance is assessed and compared to that of existing approaches. The suggested algorithm's classification performance suggests that the 5G framework could provide an accurate, rapid, reliable, and cost-effective solution to industrial automation. The structure of this article is organized as follows. The literary works related to this study, as well as the problem statement, are presented in Section II. The presented model is explained in Section III. The performance analysis of the suggested method is presented in Section IV. Finally, section V summarizes the paper's main points.

II. LITERATURE REVIEW

In **Zhang et.al (2021) [4]**, the AE approach can be used to analyze the internal fiber fracture sequence during yarn tensile fracture, providing a theoretical framework for yarn formation research. Because single fibers have varied internal macromolecular architectures, the vibration signals created during tensile

fracture have different characteristics. The deformation states of distinct single fibers can be determined using the vibration signal's characteristic scale. Singular value decomposition (SVD) of the time-frequency matrix was developed as a method for recovering AE signals generated during a single fiber tensile fracture. In this study, the EEMD and HHT were used to achieve the goal of data reduction and the building of a time-frequency matrix. The SVD method was used to minimize the characteristic dimension, allowing the typical data of vibration analysis to be more effectively reflected. To test the efficiency of extracting feature quantities by SVD, FCM cluster analysis was performed on AE signal feature quantities of distinct single fiber tensile fractures.

To achieve the more accurate capability of polyester/cotton fiber, a novel **Lu et al (2021) [5]** properly conceived and obtained suitable digital cross-section image analysis framework based on form coefficient analysis was presented. A self-developed microscopic image acquisition system was created to computerize the crossing segment of fiber. Greyscale augmentation, quantization, and open operation were among the goals of a set of image preparation methods. The edge detection method was first used to determine the fiber cross-outside section's contour. The crossing piece of the fiber was then separated using a watershed segmentation technique, and the erroneous fiber was deleted using an area elimination approach. Finally, the form correlation was used to measure whether the fibers were polyester or cotton.

A CDAN model was suggested in **Xu et.al (2021) [6]** research to optimize the effectiveness of transfer learning for spinning power usage anomaly detection. Between the element that links the source and target networks, a cluster-based adaption layer was introduced. It was created to reduce mismatches in transfer learned. The recommended CDAN model was tested in a real-world setting: a yarn spinning factory in China's Xinjiang region.

This **Agrawal et.al (2021) [7]** research looks at and offers a blockchain-based tracing architecture for multi-level cloth material and traceability of the production system. At the organizational level, it conceptualizes the interaction of supply chain partners and related network architecture, while at the operational level, it conceptualizes smart contracts and transaction validation standards. The study uses a sample of an organic-cloth-production-link that uses block-chain plus customized contracts and transformation rules to demonstrate how the proposed framework may be employed. Finally, the usefulness of the constructed block-chain is demonstrated by putting it through two tests. The proposed solution might create a distribution network partnerships' innovation trust by storing and authenticating supply chain transactions on a distributed ledger. Furthermore, the block-chain-based detecting setup will give all

partners a one-of-a-kind opportunity, flexibility, and permission to trace back their delivery system, resulting in a transparent and long-lasting supply chain.

OLES was built on a typical woven nylon cotton textile substrate in the **Arumugam et.al (2021) [8]** study. The interface layer was created by screen printing a UV curable polyurethane layer onto the textile substrate. To generate fully spray-coated flexible OLES, a way to solve spray spraying was used to deposit all of the functional layers on the textile. For process improvement, OLES devices were first produced on ITO-coated glass substrates. The OLES were then manufactured on flexible textiles using an improved spray coating method. Lastly, stencil printing epoxy was used to encase both the OLES components on the glass and fabric substrates before testing in an ambient atmosphere.

Whenever the dependent variables followed an IG distribution, the DR and PR were used to build GLM-based memory type control charts in **Amin et.al (2021) [9]** study. Comparing the performance of the suggested control charts to the GLM-based memoryless control charts in simulation research, decide which control chart delivers the overall best statistical performance in terms of ARL, SDRL, and MDRL for various types of shift sizes. The Shewhart Y-IG, CUSUM Y-IG, and EWMA Y-IG control charts outperform the Shewhart, CUSUM, and EWMA type DR-IG and PR-IG control charts in the first type of in-direct shift in mi, while the Shewhart PR-IG, CUSUM PR-IG, and EWMA PR-IG control charts outperform the Shewhart, CUSUM, and EWMA type DR-IG and The paper also suggests that, in the EWMA and CUSUM settings, using existing covariates in conjunction with the IG dispersed dependent variables can lead to a more valid conclusion.

Dai et.al (2021) [10] presents a hybrid strategy based on picture cross-correlation and the Kalman filter. The photos of the cotton flow were captured synchronously by two linear CCD cameras located at different positions. The recorded photos were then preprocessed and segmented using the linked region approach to produce separated cotton images. The coordinate transformation parameters were then calculated using image cross-correlation registration technology. The Kalman filter tracking approach was used to estimate the likely position for picture registration to speed up the process and remedy the problem when it failed. Finally, the velocity was estimated using the pixel difference between two cameras and the real distance between them. The purpose of the experiment was to verify the proposed method.

Mukai et.al (2020) [11] proposes low-frequency dielectric characteristics that are connected to their structure. At 5 distinct humidity steps, the low-frequency dielectric characteristics of cotton fibers in the

fabric thickness direction are investigated about fabric construction, thread count, and solid volume fraction (SVF). The real part of the relative permittivity is found to rise with increasing thread count, which is attributable to an increase in SVF. In excessively moist settings, however, the imaginary component of the relative permittivity and the loss tangent (dielectric loss) shows no evident monotonic tendency to the SVF. Under the regulated SVF, permittivity is shown to alter depending on fabric structures. These findings suggest that in low-frequency dielectric analysis, fabric geometrical factors, which are influenced by production processes, should be included in addition to the SVF.

The latest synthetic material for radar absorption is given in **Ayan et.al (2020) [12]** research. As a RAM, the synthetic cotton composite material was studied. Cotton fabric composites were matched to carbon fabric composites in case of mechanical and electromagnetic characteristics. In furthermore, the cotton–carbon composite combination's properties were assessed and compared to a carbon composite-only sample. Tensile and impact tests were carried out to see how the composites responded mechanically.

Yin et.al (2020) [13] examine the use of images to detect faults in a variety of applications in a variety of sectors. The Automatic Defect Identification in Fabrics design and validation was completed successfully. The current proposed system's key benefit is that it is cost-effective, enhances reliability, and lowers labor work. As a result, such technologies are extremely beneficial to the textile industry in terms of reducing personnel utilization. As a result, once applied on a broad scale, such systems can significantly reduce the costs associated with manual problem diagnosis. Another benefit of this system is that it is relatively simple and easy to understand, which has prepared the path for future enhancements.

In **Hatamie et.al (2020) [14]**, novel composite and nanoparticles have been identified as interesting candidates for improving the performance of textile-based wearable devices and optimizing the structures for intimate skin contact for improved functionality. The goal of this study is to present the most up-to-date information on chemical and physical elastic and stretchable textile-based bio-detectors, including their emergence, manufacturing, ingredients, and implementations. Aside from that, we go over some of the most recent major developments of textile-based detectors in wellness.

The goal of **Shahzad et.al (2020) [15]** was to create a blended spun yarn that is sensitively made of polymer and steel-stapled yarns, as well as to characterize its thermal behavior as a parameter of structural and procedural design. So the impact of 3 variables on the cloth's thermal behavior during testing, namely yarn twist parameter, applied voltage, and tension on the yarn, was examined. The input voltage was

determined to be the most important factor in controlling heat and thus the temperature impact of blended cloth. The yarn twisting factor, which increases the compactness of the same fineness yarn architecture at greater spinning rates. It was developed to increase the thermal impact when the twist level was increased at an applied voltage. Variations in yarn tension during the test, on the other hand, were shown to not influence yarn temperature, resulting in a consistent impact of temperature under varied tension. So this work reveals that, in addition to modifying the input-voltage, the heating impact of cloth can be increased by altering its twisting phase that regulates the compact of the cloth, allowing for the customization of different goods with specific thermal properties.

The goal of **Halepoto et.al (2019) [16]** is to present a straightforward MATLAB model for determining the actual homogeneity of neppy mélange yarn fabrics. The mélange yarn industry currently relies mainly on visual inspection and experience. However, this algorithm suggests a solution for the mélange yarn business. The proposed algorithm given in this research, which is based on kernel density function and macropixel analysis, was used to detect neps in neppy mélange yarns in real-time and calculated a 91 percent variability of neps. This method applies to the mélange yarn sector as well as other types of fashion yarns.

In **Li et.al (2019) [17],** a unique approach basis of two perpendicular CCD sensors has been devised as a basis for yarn evenness measurement. The yarn cross-sectional shape is treated as an ellipse with uneven edges and provides a system for analyzing yarn evenness using the coefficient of variation of yarn perimeter. The suggested technique's system design, algorithm flow, analytical concept, and experimental investigation are all described.

Problem Statement:

Nowadays, there are several objectives of yarn measurement like hairiness, strength, size, tensile, elasticity, etc. Deep learning, artificial intelligence, and CNN techniques are used for achieving more precision in yarn picture classification. The evaluation of yarn measurements also plays a vital role in yarn histories. So, concerning yarn measurements, this research was suggested using 5G-based TCP for the better transformation of information. By using this optimized work, accurate classification of the yarn dataset and yarn measurements were obtained.

III. PROPOSED WORK

In this article, we have proposed a novel of yarn history based on fifth-generation network technology. Initially, the yarn database is preprocessed using Grayscale transformation and image filtering methods.

Secondly, yarn segmentation is implemented using a Multi-resolution Markov Random Field (MRMRF) model. The statistical and relative features are extracted using Fourier transform and two-scale attention model respectively. We propose Improved Support Vector Machine (ISVM) classification for classifying the yarn images. The 5G network is initialized and Transmission Control Protocol is used for data transfer. To enhance the performance we propose an IPSO algorithm. The performance of the suggested methodology is analyzed and compared with existing methodologies using the MATLAB simulation tool. The classification performance of the suggested algorithm indicates that the 5G framework might provide an accurate, fast, reliable, and cost-effective solution to industrial automation. Figure.1 points to the representation of the proposed structure.

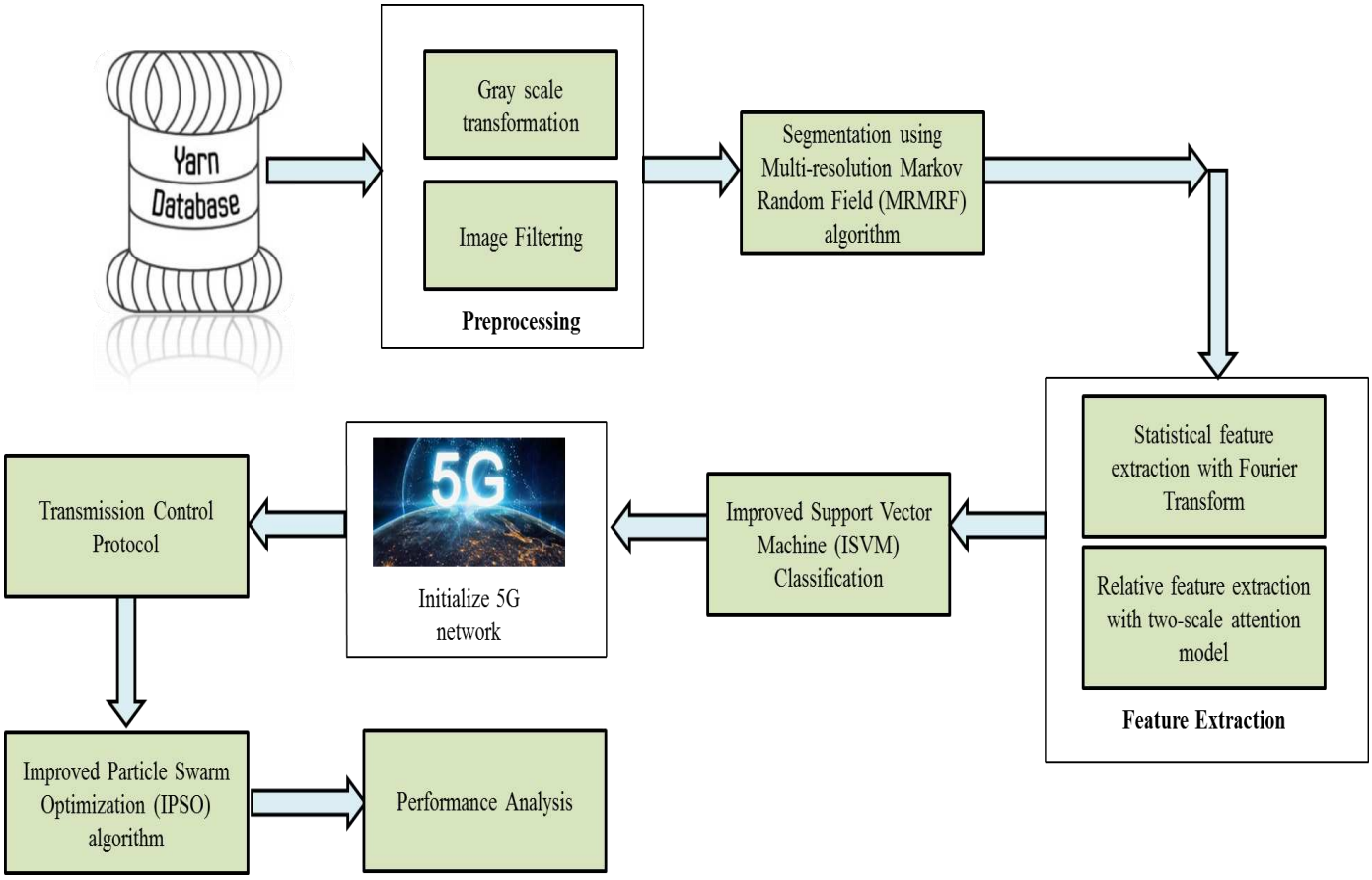

Figure 1. Representation of proposed structure

Yarn Database:

The yarn sheet winder forms and winds a sample of fabric/yarn (cloth) on a chalkboard in line with ASTM D2255, the norm. The scanner was used in this investigation to obtain a digital yarn board image. The cloth sheet model is matched to photography-based flow norms showing various results to objectively judge the

effectiveness of cloth model based on resemblance among both the cloth model and ordinary picture in the conventional method. The normal image size is 9.5*5.5 inches wide by 5.5 inches tall (52.25 inch2). The dimension of the digitalized cloth picture is fixed at 7*7 (inches) to maintain a comparable number of cloth data of match (49 inches 2). The digitalized color cloth photos in this study were captured with a Cano Scan 8800F scanner that has a pixel of 500(dpi) and a size of 7*7 inches.

Image Pre-processing using grayscale transformation and image filtering:

Image preprocessing is used to enhance the contrast and boost the precision of the yarn's measurement. Pre-processing stage in this work essentially comprises of following steps: grayscale transformation and picture filtration. The initial stage, which converts color photos to grey images, is simple to accomplish. Due to the effect of the image setting and settings, picture noises are inescapable. As a result, the photos must be filtered following grayscale transformation. Salt and pepper noise can be suppressed using traditional average and median filtering algorithms; however, features in the picture were readily inconvenienced. This research uses an enhanced filter technique called the Mean Merged Median Filtering Algorithm (MMMFA), which merges mean and median filtering. To begin, image noise was removed using an enhanced average filtering technique. In this enhanced pixel discard strategy, the grey value of the item image will be summed unless the variance between its real value and the mean value of its nearby pixels is greater than a predefined threshold; otherwise, the measurement of this pixel point will not be modified. Whenever reducing noise, the method used retains the clarity of the images to the greatest extent possible.

The middle grey amount of pixels ordered in a filtered level for the approved pixel is used in traditional median filtering, although the pixels in the level are not always with the pixel you've chosen. As a result, if a characteristic field in the picture is little, there may be no mid-value within the filter window, and this area is at risk of being filtered out incorrectly. Similarly, before imposing the median filter, we establish a threshold to avoid losing details. As a result, if the difference between the grey value and the median value is less than the threshold, only one pixel's grey value will not be changed by the median value. Because their grey values are prone to deviating greatly from those of the surrounding pixels, the chosen approach is excellent in filtering out outliers generated by sounds. By using the histogram equalization method, we may improve the yarn picture after filtering to show the corner frame data of the yarn.

Segmentation using Multi-resolution Markov Random Field (MRMRF) algorithm:

Purposely $B = \{B_1, B_2, B_3, \ldots . . B_m\}$ expresses the aspect area which points to the yarn picture, $b = \{b_1, b_2, b_3, \ldots . . b_m\}$ represents the originality of the aspect area. Domineering $A = \{A_1, A_2, \ldots . . A_m\}$ represents the label area that points to the segmentation outputs of yarn picture, $a = \{a_1, a_2, \ldots . . a_m\}$ represents the originality of label area and a type of segmentation output.

$a_r \in S = \{1,2, \ldots l\}$,

Where r = 1, 2,….m and m=M^2

S = phase space in the label area

l=number of different label categories

Picture of a yarn B is defined on the grid G, which has Mp wavebands and is of size M*M.

B realizes C-1 layers wavelet decomposition, with sc($1 \leq sc \leq C\text{-}1$) representing the level number of every wavelet scale.

D, a decomposition set, contains wavelet coefficients set $D^{(d)}$ ($d \in \{1,2, \ldots Mp\}$) that is associated with Mp wavebands. The lowest quality is sc = C-1, which comprises the wavelet coefficients of 4 bands (LL, LH, HL, HH) and Mp wavebands, while the others are sc($1 \leq sc \leq C\text{-}1$), which includes 3 bands (LH, HL, HH) wavelet components and Mp wavebands.

The actual yarn picture is shown in this article with the quality matching to level sc is zero. As a result, C-1 layers wavelet decomposition is used to create digital picture series of C various resolutions.

Considering grid $G_s = \{ (i, j); 1 \leq i \leq (M/2^s), 1 \leq C \leq (M/2^s) \}$ is depicted in the scale $sc \in \{0, 1, ..., C - 1\}$. The location of any pixel (i, j) on grid Gs can then be written as r′, which is a number between 1 and m′. Also, $m' = (M/2^s)^2$.

On the biggest scale, sc = C-1, a feature vector is given in equation (1).

$$D_{r'}^{sc} = \left[D_{r'}^{(sc)(1)}, D_{r'}^{(sc)(2)}, \ldots, D_{r'}^{(sc)(d)}, \ldots, D_{r'}^{(sc)(d)}\right]^T \quad (1)$$

Where

$$D_{m'}^{(sc)(d)} = \left[D_{r'}^{(sc)(d)(LL)}, D_{r'}^{(sc)(d)(LH)}, D_{r'}^{(sc)(d)(HL)}, D_{r'}^{(sc)(d)(HH)}\right] \quad (2)$$

In equation (2), $D_{r'}^{(sc)(d)(LL)}, D_{r'}^{(sc)(d)(LH)}, D_{r'}^{(sc)(d)(HL)}, D_{r'}^{(sc)(d)(HH)}$ are wavelet coefficients in position r′ of every band in the scale sc on d wave band, accordingly. It should be noticed that on the scale sc($1 \leq sc \leq C-2$), there is no wavelet component of the LL band of the feature space.

Feature extraction using statistical and relative methods:

The approach and principle of operation for extracting the features will be detailed in this part. The raw yarn board picture may be used to obtain the quality of the yarn picture. The statistical properties of all the yarn samples can then be retrieved and fed into PNN to categorize the yarn surface look grades.

Statistical features extraction with Fourier Transform:

The yarns platform picture is first divided into yarn images to acquire these statistics. After some statistical parameters have been recovered, Fourier processing, thresholding, and post-processing can also be used to measure the yarn diameter for further study. Cotton strands have a high-frequency component in the FFT band, whereas the yarn body has a reduced component. The bulk of yarn hairs can be removed using a Butterworth low-pass filter (BLPF), which can be described in equation (3).

$$\mathrm{M(a,b)} = \frac{1}{1+[\mathrm{L(a,b)}/\mathrm{L_0}]^{2\mathrm{m}}} \tag{3}$$

L(a, b) is the frequency domain distance between a point (a, b) and the origin, L_0 is the distance between starting and cut-off range frequencies, and m is denoted as an order of BLF.

The average score of measurements of cloth is retrieved as an aspect g_1 of yarn number for assessment depends upon he cloth measurement derived from the yarn self-picture as shown in equation (4).

$$g_1 = a_m = \frac{1}{l}\sum_{j=1}^{l} a_j \tag{4}$$

Where, l = entire length in pixels

a_j = yarn's j-th diameter

a_m = mean value of the diameter

To evaluate the variability in yarn diameter, the coefficient of variation (C), g_2, is derived in equation (5).

$$g_2 = C = \frac{\sqrt{\frac{1}{l}\sum_{j=1}^{m}(a_j - a_m)^2}}{\frac{1}{l}\sum_{j=1}^{m} a_j} \tag{5}$$

And g_3 is determined in equation (6) as a percentage of thick regions compared to yarn length.

$$g_3 = \frac{t_r}{l} \tag{6}$$

Here, g_4, is determined in equation (7) as a percentage of thin regions compared to yarn length.

$$g_4 = \frac{No.of\ thin\ regions}{l} \quad (7)$$

Here, g_5, is determined in equation (8) as a percentage of neps compared to yarn length.

$$g_5 = \frac{No.of\ neps}{l} \quad (8)$$

The Skewness of yarn derived in equation (9) as,

$$g_6 = \frac{\frac{1}{m}\sum_{j=1}^{m}(a_j - a_m)^3}{\left(\sqrt{\frac{1}{m}\sum_{j=1}^{m}(a_j - a_m)^2}\right)^3} \quad (9)$$

Kurtosis is a metric for determining how peaked or flat a distribution is shown in equation (10).

$$g_7 = \frac{\frac{1}{m}\sum_{j=1}^{m}(a_j - a_m)^4}{\left(\frac{1}{m}\sum_{j=1}^{m}(a_j - a_m)^2\right)^2} \quad (10)$$

Determining the degree of unpredictability in hairiness as shown in equation (11).

$$g_8 = -\sum_{r=0}^{K-1}(p \times log_2 p) \quad (11)$$

Here p is the probability linked with grey level r, and K denotes the no. of grey levels in the picture,

Relative feature extraction with two-scale attention model:

Yet, the picture's dots per inch have not been properly examined in current attention theories as a practical concern. Many attention models work well with images with low DPI, while others work well with images with high DPI. Furthermore, the resultant saliency patterns differ dramatically when a two-attention model is applied to 2 pictures in addition to various DPIs generated from the same yarn sheet. As a result, determining an appropriate DPI is critical to extract precise characteristics for measuring the important regions.

The equation (12) for the link between visual range v and picture quality q is,

$$q = \frac{1}{2 \times v \times tan\frac{\tau}{2}} \quad (12)$$

Where τ = human eye's smallest distinct angle and $\frac{v_1}{v_2} = \frac{q_2}{q_1}$.

Classification using Improved Support Vector Machine (ISVM) classifier:

The improved SVM classifiers were created with binary categorization in mind. The categorization uses a combination of features as inputs and quantitative corresponding labels as outputs to target different types of visual defects.

In equation (13), the SVM requires the calculation of the following optimal solution given the training-vector $t_j \in K^m$, j=1,2,..,r and label vector $v \in K^r$, $v_j \in [1, -1]$.

$$\begin{aligned} &\min_{e,f,g} \frac{1}{2} e^T e + c \sum_{j=1}^{r} g_j \\ s.t.\ \ &v_i\left(e^T \theta(t_j) + f\right) \geq 1 - g_j, g_j = \geq 0. \end{aligned} \tag{13}$$

The variable θ is used to translate the training vector t_j into a higher-dimensional space. In a higher-dimensional space, SVM locates a linear dividing hyperplane with the greatest margin. And f is the constant term, and e is the normal vector of the hyper-plane. [c > 0] denotes the error phrase's penalty variable, and g_j denotes the class outcomes' fault vector. Additionally, the Kernel function (KF) can be defined as $KF(t_j, v_q)$.

The radial basis function (RBF) is employed in this study as shown in equation (14).

$$KF\left(t_j, t_q\right) = exp\left(-\delta \left|\left|t_j - t_q\right|\right|^2\right),\ \delta > 0 \tag{14}$$

The kernel variable is denoted by δ.

The RBF illustrates the associations between both the training and testing data sources (t_j and t_q) respectively. This kernel may non-linearly translate the examples into a higher-dimensional space and manage the circumstance when the attribute-class label relationship is nonlinear. Furthermore, the RBF kernel outperforms other non-linear functions in terms of computational quality.

Initialize 5G network:

Although 5G networks and research and refers are now in progress, the deployment of commercialized 5G internet infrastructure will demand the provision of monitoring solutions at 5G networks I&M to assure IPE functionality. As a consequence, we'll need to set up a high-speed 5G network to transmit data goodness.

Transmission Control Protocol:

TCP (Transmission Control Protocol) is a protocol for establishing and maintaining a network dialogue in which services can transfer messages. TCP is used in conjunction with the Internet Protocol (IP), which specifies how computers exchange packets of data. TCP and IP are the fundamental rules that govern the

network. TCP carries out the following tasks: analyzes how to divide application packets of data that network can transport; sends and receives network packet; manages to flow; controls restoration of lost or corrupted packets to enable error-free data transfer, and recognizes all messages that come.

Improved particle swarm optimization (IPSO) algorithm:

A particle has been used to replicate the above-mentioned solo bird in the IPSO method, and each atom may be viewed as a searching individual in the N-dimensional search space. The particle's present position is determined based on the relevant optimization issue, and the particle's flight symbolizes the individual's search strategy. The particle's flying speed can be dynamically modified based on the particle's historic optimal location and the population's historic optimum position. Particles simply have two characteristics: speed and location. The pace of movement is represented by speed, whereas the direction of movement is represented by position. The individual extreme is the best individual extreme in the particle population, and the present global optimization model is the greatest individual extreme in the particle community. Iterate continually, using equations (15) and (16) to update the speed and position, until you reach the best solution to meet the terminate requirement.

$$s_j = I\, s_j + a_1 rand(0,1)\left(q_j - y_j\right) + a_2 rand(0,1)\left(q_g - y_j\right) \quad (15)$$

$$y_j = y_j + s_j \quad (16)$$

In d-dimension,

y_j = position of j-th particle

s_j = speed of j-th particle

I = inertia (non-negative value)

q_j = individual extreme of j-th particle

q_g = global optimization solution.

If y_j is lower, the capability is poorer in global searching but higher in local searching. The global and local search effectiveness can both be improved by altering the value of y_j.

Here a1 and a2 are represent signify speed coefficients, with the former serving as each particle's independent learning factor and the latter as every particle's socialization component.

IV. PERFORMANCE ANALYSIS

The Matlab/Simulink tool is used to evaluate the research method. The behavior of the proposed technique has been evaluated in terms of accuracy, throughput, makespan, and energy utilization.

Accuracy:

It determines how many data are successfully classified. It determines how closely the outcomes correspond to the desired objective. It is denoted by A as shown in equation (17).

$$A = \frac{TP+TN}{TP+TN+FP+FN} \quad (17)$$

The pixel counts that the program correctly detects as positive are referred to as TP. The pixel numbers that the system correctly detect as negative are referred to as TN. The pixel can be counted that are identified as positive, but not exactly are known as FP. The pixel numbers that are recognized as negative but just not the precise ones are referred to as FN.

- ❖ TP indicates that a black fungus is present and has been correctly diagnosed.
- ❖ TN indicates that the black fungus is not present and has not been identified.
- ❖ FP indicates that a black fungus is not present but has been identified.
- ❖ FN denotes the presence of a black fungus that has yet to be identified.

We also compare the proposed strategy to a few other methods for calculating these values.

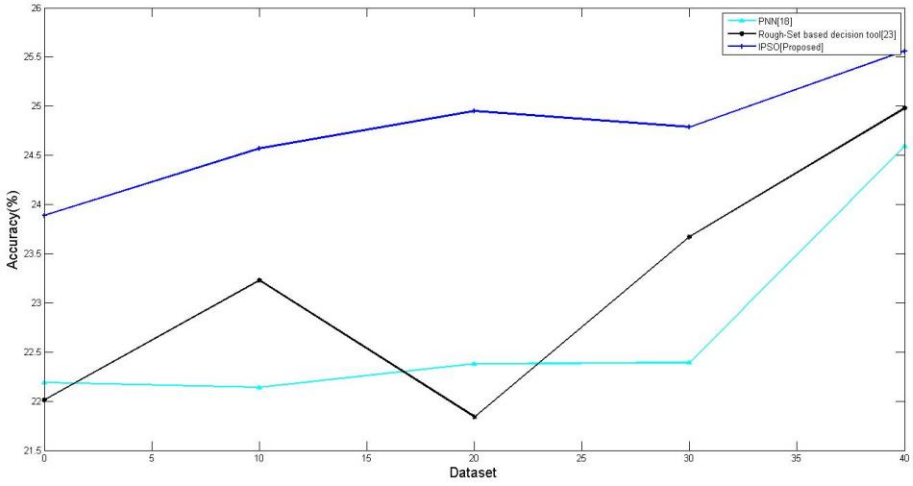

Figure 2: Comparison of Accuracy (%) with suggested and existing methods

The accuracy of the existing and suggested approaches is compared in Figure 2. The graph clearly shows that the proposed technique is more accurate than the existing one.

Throughput:

At any given time, it is the total number of packets transferred over the network from sender nodes to reception nodes. It's commonly measured in bits per second or packets per second. The throughput must be comparable to attain better results. The value of throughput is calculated using Equation (18).

$$Throughput = \frac{Rpackets}{Rlast - Rstart} \quad (18)$$

Where $R_{packets}$ = received packets

R_{last} = last or end packet

R_{start} = starting packet

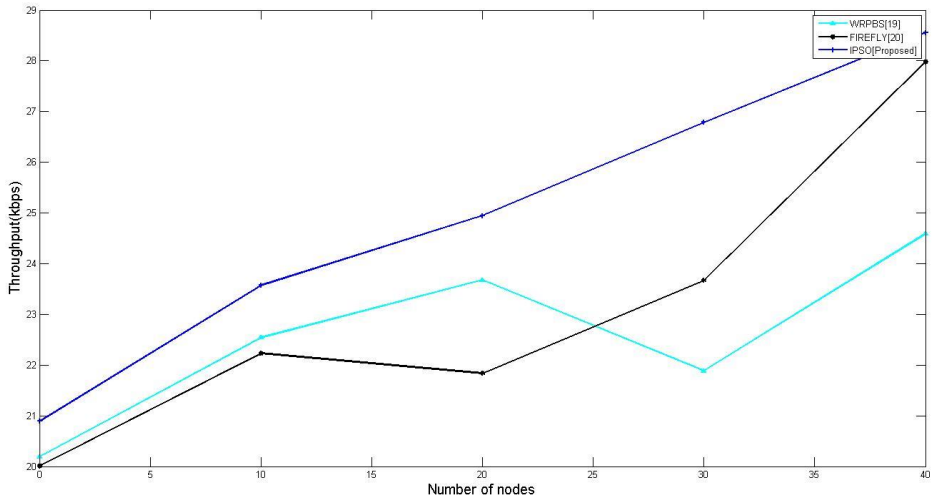

Figure 3: Comparison of throughput (kbps) with suggested and existing methods

Figure 3 compares the throughput of the existing and suggested methodologies. The plot clearly illustrates that the suggested technique has more throughput rate than existing methods.

Makespan:

Makespan is the time it takes for a project to complete from start to finish. This sort of multi-mode resource-restricted task scheduling challenge aims to construct the shortest conceptual project timeline feasible by efficiently utilizing project resources and adding the fewest additional resources possible to achieve the smallest makespan conceivable. In the context of scheduling, the term is frequently used.

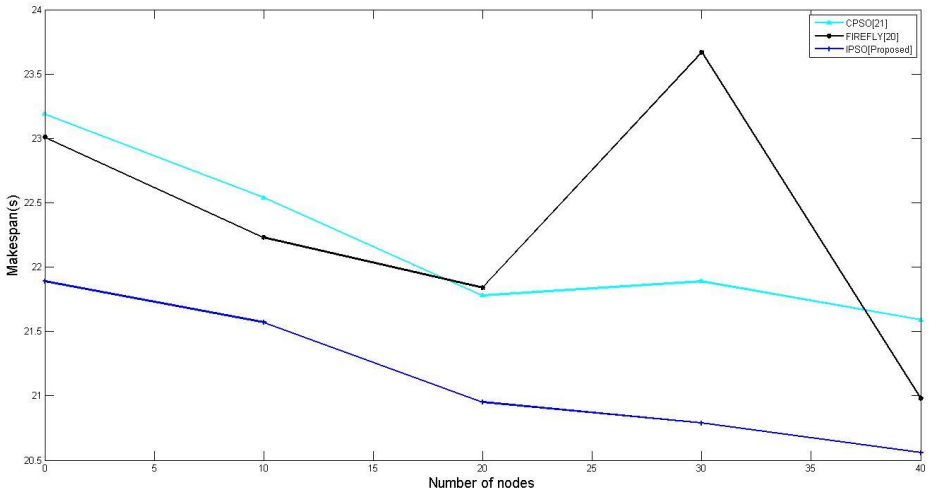

Figure 4: Comparison of makespan(s) with suggested and existing methods

Figure 4 shows a comparison of the makespan (in seconds) of the existing and proposed methodologies. The graph demonstrates that the proposed technique has lessened makespan than existing techniques.

Energy utilization:

ICT (Information and Communication Technology) engine's energy usage is quickly increasing, posing a huge economic and ecological challenge. The biggest amount of energy is consumed during the consumption period, as per the life-cycle analysis of switch ports. In this study, we can achieve minimization of energy utilization by using the IPSO technique that is used for improving the rate of transmission of data.

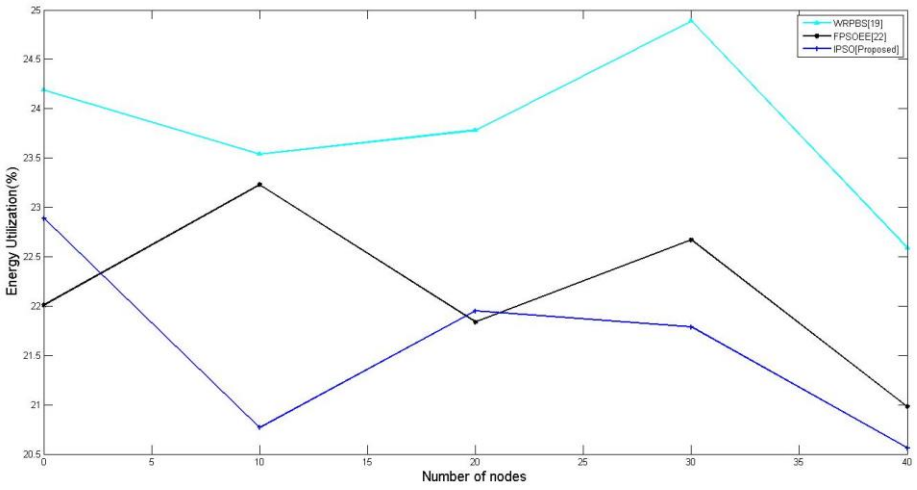

Figure 5: Comparison of Energy utilization (%) with suggested and existing methods

Figure 5 shows a comparison of the energy utilization of the existing and proposed methodologies. The graph demonstrates that the proposed technique utilizes a little amount of energy than existing techniques.

V. CONCLUSION

This paper proposes the development and application of information resources for the education and teaching of yarn history based on fifth-generation (5G) network technologies. In this paper, the collected dataset was pre-processed by two methods that are grayscale transformation method and the filtering method. The grayscale transformation method is used to transform or change any color into gray color which illustrates the location of any fault. Then filtering method can be used for filters the unwanted things on the image for the achievement of a better accurate or virtue or goodness resolution image. Here, the aspects were extracted using both the statistical extraction with the Fourier Transform model and relative extraction with the two-scale attention model. Then feature classification can be done by the ISVM classifier to get the images with better filtering. Nowadays, 5G network plays a vital role in the whole network world. So main aim of this paper is to optimize the data transfer rate that means enhancement of TCP for better performance will achieved. Improved particle swarm optimization algorithm used to optimize the TCP which is to be connected with 5G network setup. Finally, the assessment concerning the accuracy, throughput, makespan and energy utilization can be obtained and the result was verified in the MATLAB software tool.

Funding Information: The year 2018-2019 Fundamental Research Funds for the Central Universities and Graduate Student Innovation Fund of Donghua University “Research on the development of sizing technology in China” (Project No., CUSF-DH-D-2019105) stage of achievements.

REFERENCE

1. Yagihara, S., Saito, H., Sugimoto, H., Kawaguchi, T., Fukuzaki, M., Igarashi, T., Hoshi, M. and Nakamura, K., 2021. Evaluation of water structures in cotton cloth by fractal analysis with broadband dielectric spectroscopy. Journal of Materials Science, 56(31), pp.17844-17859.
2. Atalie, D., Gideon, R.K., Ferede, A., Tesinova, P. and Lenfeldova, I., 2021. Tactile comfort and low-stress mechanical properties of half-bleached knitted fabrics made from cotton yarns with different parameters. Journal of Natural Fibers, 18(11), pp.1699-1711.
3. Sayeed, M.A., Schumann, M., Wanjura, J., Kelly, B.R., Smith, W., and Hequet, E.F., 2021. Characterizing the total within-sample variation in cotton fiber length using the High Volume Instrument fibrogram. Textile Research Journal, 91(1-2), pp.175-187.

4. Zhang, X., Xin, B., Zheng, Y., Shi, M., Lin, L., Gao, C., Yi, Y., Yang, Z., and Li, H., 2021. Study on fiber fracture sequence during yarn tensile fracture via acoustic emission method. The Journal of The Textile Institute, 112(3), pp.417-428.
5. Lu, S., Deng, N., Xin, B., Wang, Y. and Wang, W., 2021. Investigation on Image-Based Digital Method for Identification on Polyester/Cotton Fiber Category. Fibers and Polymers, 22(6), pp.1774-1783.
6. Xu, C., Wang, J., Zhang, J., and Li, X., 2021. Anomaly detection of power consumption in yarn spinning using transfer learning. Computers & Industrial Engineering, 152, p.107015.
7. Agrawal, T.K., Kumar, V., Pal, R., Wang, L., and Chen, Y., 2021. Blockchain-based framework for supply chain traceability: A case example of textile and clothing industry. Computers & industrial engineering, 154, p.107130.
8. Arumugam, S., Li, Y., Pearce, J., Charlton, M.D., Tudor, J., Harrowven, D., and Beeby, S., 2021. Spray-Coated Organic Light-Emitting Electrochemical Cells Realized on a Standard Woven Polyester Cotton Textile. IEEE Transactions on Electron Devices, 68(4), pp.1717-1722.
9. Amin, M., Mahmood, T. and Kinat, S., 2021. Memory type control charts with the inverse-Gaussian response: An application to the yarn manufacturing industry. Transactions of the Institute of Measurement and Control, 43(3), pp.656-678.
10. Dai, Y., Xu, T., Feng, Z., and Gao, X., 2021. Cotton flow velocity measurement based on image cross-correlation and Kalman filtering algorithm for foreign fiber elimination. The Journal of The Textile Institute, pp.1-8.
11. Mukai, Y., Dickey, E.C. and Suh, M., 2020. Low-frequency dielectric properties related to the structure of cotton fabrics. IEEE Transactions on Dielectrics and Electrical Insulation, 27(1), pp.314-321.
12. Ayan, M.Ç., Kiriş, S., Yapici, A., Karaaslan, M., Akgöl, O., Altıntaş, O. and Ünal, E., 2020. Investigation of cotton fabric composites as a natural radar-absorbing material. Aircraft Engineering and Aerospace Technology.
13. Yin, S., Bao, J., Zhang, J., Li, J., Wang, J., and Huang, X., 2020. Real-time task processing for spinning cyber-physical production systems based on edge computing. Journal of Intelligent Manufacturing, 31(8).
14. Hatamie, A., Angizi, S., Kumar, S., Pandey, C.M., Simchi, A., Willander, M., and Malhotra, B.D., 2020. Textile-based chemical and physical sensors for healthcare monitoring. Journal of the Electrochemical Society, 167(3), p.037546.

15. Shahzad, A., Jabbar, A., Irfan, M., Qadir, M.B., and Ahmad, Z., 2020. Electrical resistive heating characterization of conductive hybrid staple spun yarns. The Journal of the Textile Institute, 111(10), pp.1481-1488.
16. Halepoto, H., Gong, T. and Kaleem, K., 2019. Real-Time Quality Assessment of Neppy Mélange Yarn Manufacturing Using Macropixel Analysis. Textiles, 62(4).
17. Li, G., Akankwasa, N.T., Zhao, Q. and Wang, J., 2019. A novel system for yarn cross-section analysis based on dual orthogonal CCD sensors. Journal of Natural Fibers, 16(1), pp.114-125.
18. Li, S.Y., Xu, B.G., Fu, H., Tao, X.M. and Chi, Z.R., 2018. A two-scale attention model for intelligent evaluation of yarn surface qualities with computer vision. The Journal of the Textile Institute, 109(6), pp.798-812.
19. Tabibi, S. and Ghaffari, A., 2019. Energy-efficient routing mechanism for a mobile sink in wireless sensor networks using particle swarm optimization algorithm. Wireless Personal Communications, 104(1), pp.199-216.
20. Golchi, M.M., Saraeian, S. and Heydari, M., 2019. A hybrid of firefly and improved particle swarm optimization algorithms for load balancing in cloud environments: Performance evaluation. Computer Networks, 162, p.106860.
21. Jacob, T.P. and Pradeep, K., 2019. A multi-objective optimal task scheduling in cloud environment using cuckoo particle swarm optimization. Wireless Personal Communications, 109(1), pp.315-331.
22. Robinson, Y.H., Balaji, S. and Julie, E.G., 2019. FPSOEE: Fuzzy-enabled particle swarm optimization-based energy-efficient algorithm in mobile ad-hoc networks. Journal of Intelligent & Fuzzy Systems, 36(4), pp.3541-3553.
23. Das, S. and Ghosh, A., 2021. Rough Set-Based Decision Tool for Classification of Cotton Yarn Neps. Journal of The Institution of Engineers (India): Series E, 102(1), pp.1-10.